

8. Velazquez-Perez L, Rodriguez-Labrada R, Gonzalez-Garces Y, et al. Prodromal spinocerebellar ataxia type 2 subjects have quantifiable gait and postural sway deficits. *Mov Disord* 2021;36(2):471–480.
9. Zhou H, Nguyen H, Enriquez A, et al. Assessment of gait and balance impairment in people with spinocerebellar ataxia using wearable sensors. *Neurol Sci* 2022;43(4):2589–2599. <https://doi.org/10.1007/s10072-021-05657-6>
10. Ilg W, Schatton C, Schicks J, Giese MA, Schols L, Synofzik M. Video game-based coordinative training improves ataxia in children with degenerative ataxia. *Neurology* 2012;79(20):2056–2060.
11. Ilg W, Christensen A, Mueller OM, Goericke SL, Giese MA, Timmann D. Effects of cerebellar lesions on working memory interacting with motor tasks of different complexities. *J Neurophysiol* 2013;110(10):2337–2349.
12. Serrao M, Pierelli F, Ranavolo A, et al. Gait pattern in inherited cerebellar ataxias. *Cerebellum* 2012;11(1):194–211.
13. Wuehr M, Schniepp R, Ilmberger J, Brandt T, Jahn K. Speed-dependent temporospatial gait variability and long-range correlations in cerebellar ataxia. *Gait Posture* 2013;37(2):214–218.
14. Rochester L, Galna B, Lord S, Mhiripiri D, Eglon G, Chinnery PF. Gait impairment precedes clinical symptoms in spinocerebellar ataxia type 6. *Mov Disord* 2014;29(2):252–255.
15. Hickey A, Gunn E, Alcock L, et al. Validity of a wearable accelerometer to quantify gait in spinocerebellar ataxia type 6. *Physiol Meas* 2016;37(11):N105–N117.
16. Schniepp R, Wuehr M, Schlick C, et al. Increased gait variability is associated with the history of falls in patients with cerebellar ataxia. *J Neurol* 2014;261(1):213–223.
17. Janse RJ, Hoekstra T, Jager KJ, et al. Conducting correlation analysis: important limitations and pitfalls. *Clin Kidney J* 2021;14(11):2332–2337.
18. Schmitz-Hübsch T, du Montcel ST, Baliko L, et al. Scale for the assessment and rating of ataxia: development of a new clinical scale. *Neurology* 2006;66(11):1717–1720.
19. Schmitz-Hübsch T, Coudert M, Bauer P, et al. Spinocerebellar ataxia types 1, 2, 3, and 6: disease severity and nonataxia symptoms. *Neurology* 2008;71(13):982–989.
20. Muller B, Ilg W, Giese MA, Ludolph N. Validation of enhanced Kinect sensor based motion capturing for gait assessment. *PLoS One* 2017;12(4):e0175813.
21. Schniepp R, Wuehr M, Neuhaeuser M, et al. Locomotion speed determines gait variability in cerebellar ataxia and vestibular failure. *Mov Disord* 2012;27(1):125–131.
22. Ilg W, Fleszar Z, Schatton C, et al. Individual changes in preclinical spinocerebellar ataxia identified via increased motor complexity. *Mov Disord* 2016;31(12):1891–1900.
23. Winter DA. *Biomechanics and Motor Control of Human Gait: Normal, Elderly and Pathological*. 2nd ed. Waterloo, Canada: Wiley-Interscience Publication; 1991.
24. Cliff N. Answering ordinal questions with ordinal data using ordinal statistics. *Multivar Behav Res* 1996;31(3):331–350.
25. Kerby DS. The simple difference formula: an approach to teaching nonparametric correlation. *Compr. Psychiatry* 2014;3:11.IT.13.11.
26. Tezenas du Montcel S, Durr A, Rakowicz M, et al. Prediction of the age at onset in spinocerebellar ataxia type 1, 2, 3 and 6. *J Med Genet* 2014;51(7):479–486.
27. Faul F, Erdfelder E, Buchner A, Lang AG. Statistical power analyses using G\*power 3.1: tests for correlation and regression analyses. *Behav Res Methods* 2009;41(4):1149–1160.
28. Globas C, du Montcel ST, Baliko L, et al. Early symptoms in spinocerebellar ataxia type 1, 2, 3, and 6. *Mov Disord* 2008;23(15):2232–2238.
29. Ilg W, Branscheidt M, Butala A, et al. Consensus paper: neurophysiological assessments of ataxias in daily practice. *Cerebellum* 2018;17(5):628–653.
30. Klockgether T, Mariotti C, Paulson HL. Spinocerebellar ataxia. *Nat Rev Dis Primers* 2019;5(1):24.
31. Buckley E, Mazza C, McNeill A. A systematic review of the gait characteristics associated with cerebellar ataxia. *Gait Posture* 2018;60:154–163.
32. Ilg W, Timmann D. Gait ataxia-specific cerebellar influences and their rehabilitation. *Mov Disord* 2013;28(11):1566–1575.
33. Jacobi H, du Montcel ST, Bauer P, et al. Long-term disease progression in spinocerebellar ataxia types 1, 2, 3, and 6: a longitudinal cohort study. *Lancet Neurol* 2015;14(11):1101–1108.
34. Diallo A, Jacobi H, Tezenas du Montcel S, Klockgether T. Natural history of most common spinocerebellar ataxia: a systematic review and meta-analysis. *J Neurol* 2021;268(8):2749–2756.
35. Manta C, Patrick-Lake B, Goldsack JC. Digital measures that matter to patients: a framework to guide the selection and development of digital measures of health. *Digit Biomark* 2020;4(3):69–77.
36. Wilke C, Haas E, Reetz K, et al. Neurofilaments as blood biomarkers at the preataxic and ataxic stage of spinocerebellar ataxia type 3: a cross-species analysis in humans and mice. *medRxiv* 2020;12(7):e11803. <https://doi.org/10.15252/emmm.201911803>
37. Faber J, Schaprian T, Berkan K, et al. Regional brain and spinal cord volume loss in spinocerebellar ataxia type 3. *Mov Disord* 2021;36(10):2273–2281.
38. Cabaraux P, Agrawal SK, Cai H, et al. Consensus paper: ataxic gait. *Cerebellum* 2022;12. <https://doi.org/10.1007/s12311-022-01373-9>. Online ahead of print.
39. Thierfelder A, Seemann J, John N, et al. Real-life turning movements capture subtle longitudinal and preataxic changes in cerebellar ataxia. *Mov Disord* 2022;37(5):1047–1058.

## Supporting Data

Additional Supporting Information may be found in the online version of this article at the publisher's web-site.

## Serotonin Transporter Imaging in Multiple System Atrophy and Parkinson's Disease

Kelvin L. Chou, MD,<sup>1,2\*</sup> Praveen Dayalu, MD,<sup>1</sup> Robert A. Koeppe, PhD,<sup>3</sup> Sid Gilman, MD,<sup>1</sup> C. Chauncey Spears, MD,<sup>1</sup> Roger L. Albin, MD,<sup>1,2,4,5</sup> and Vikas Kotagal, MD, MS<sup>1,3</sup>

This is an open access article under the terms of the Creative Commons Attribution License, which permits use, distribution and reproduction in any medium, provided the original work is properly cited.

\*Correspondence to: Dr. Kelvin L. Chou, Department of Neurology, University of Michigan, Ann Arbor, MI 48109, USA; E-mail: klchou@med.umich.edu

Relevant conflicts of interest/financial disclosures: Nothing to report.

Funding agencies: National Institutes of Health Grants P01NS044233, R56NS082941, R56AG065529, P50NS123067, and R01AG065246 and the Parkinson's Foundation.

Received: 15 April 2022; Revised: 10 August 2022; Accepted: 18 August 2022

Published online 14 September 2022 in Wiley Online Library (wileyonlinelibrary.com). DOI: 10.1002/mds.29220

<sup>1</sup>Department of Neurology, University of Michigan, Ann Arbor, Michigan, USA <sup>2</sup>University of Michigan Udall Center, Ann Arbor, Michigan, USA <sup>3</sup>Division of Nuclear Medicine, Department of Radiology, University of Michigan, Ann Arbor, Michigan, USA <sup>4</sup>Veterans Affairs Ann Arbor Health System (VAAAHS) and VAAAHS Geriatric Research Education and Clinical Center, Ann Arbor, Michigan, USA <sup>5</sup>University of Michigan Parkinson's Foundation Research Center of Excellence, Ann Arbor, Michigan, USA

**ABSTRACT: Background:** Both Parkinson's disease (PD) and multiple system atrophy (MSA) exhibit degeneration of brainstem serotonergic nuclei, affecting multiple subcortical and cortical serotonergic projections. In MSA, medullary serotonergic neuron pathology is well documented, but serotonin system changes throughout the rest of the brain are less well characterized.

**Objectives:** To use serotonin transporter [<sup>11</sup>C]3-amino-4-(2-dimethylaminomethyl-phenylsulfaryl)-benzonitrile positron emission tomography (PET) to compare serotonergic innervation in patients with MSA and PD.

**Methods:** We performed serotonin transporter PET imaging in 18 patients with MSA, 23 patients with PD, and 16 healthy controls to explore differences in brainstem, subcortical, and cortical regions of interest.

**Results:** Patients with MSA showed lower serotonin transporter distribution volume ratios compared with patients with PD in the medulla, raphe pontis, ventral striatum, limbic cortex, and thalamic regions, but no differences in the dorsal striatal, ventral anterior cingulate, or total cortical regions. Controls showed greater cortical serotonin transporter binding compared with PD or MSA groups but lower serotonin transporter binding in the striatum and other relevant basal ganglia regions. There were no regional differences in binding between patients with MSA-parkinsonian subtype ( $n = 8$ ) and patients with MSA-cerebellar subtype ( $n = 10$ ). Serotonin transporter distribution volume ratios in multiple different regions of interest showed an inverse correlation with the severity of Movement Disorders Society Unified Parkinson's Disease Rating Scale motor score in patients with MSA but not patients with PD.

**Conclusions:** Brainstem and some forebrain subcortical region serotonergic deficits are more severe in MSA compared with PD and show an MSA-specific correlation with the severity of motor impairments. © 2022 The Authors. *Movement Disorders* published by Wiley Periodicals LLC on behalf of International Parkinson and Movement Disorder Society.

**Key Words:** multiple system atrophy; serotonin; [<sup>11</sup>C]DASB; PET imaging; Parkinson disease

Dysfunction of caudal brainstem serotonergic raphe nuclei is suggested to occur early in Parkinson's disease (PD).<sup>1</sup> The relative frailty of these nuclei in PD may

relate to their high baseline metabolic activity<sup>2</sup> or their key role in interconnected brainstem projection system networks<sup>3</sup> implicated in the cell-to-cell spread of misfolded synuclein. Multiple system atrophy (MSA) is a parkinsonian disorder with neuronal cell loss in several neurotransmitter projection systems.<sup>4</sup> There are two clinical subtypes of MSA: a parkinsonian subtype (MSA-P), presenting primarily with parkinsonism, and a cerebellar subtype (MSA-C), presenting as a progressive cerebellar disorder with later expression of parkinsonism. MSA is characterized by glial cytoplasmic synuclein pathology rather than the neuron inclusions characteristic of PD.<sup>5</sup> There is clear neuropathologic evidence of serotonergic neuronal loss in the caudal brainstem raphe nucleus complex in MSA.<sup>6,7</sup> These neurons are known to project within the caudal brainstem and to motor and intermediolateral areas of the spinal cord. Their degeneration may contribute to MSA-specific features, including respiratory and autonomic dysfunction.

We know less about the extent of rostral serotonergic projection system degeneration in MSA compared with PD. Rostral serotonergic projections to the striatum, thalamus, and limbic cortices are implicated in PD as risk factors for sleep difficulties,<sup>8</sup> affective symptoms,<sup>9</sup> and weight changes.<sup>10</sup> Similar nonmotor features are common and severe in MSA,<sup>11</sup> although their biological basis is less well understood. [<sup>11</sup>C]3-amino-4-(2-dimethylaminomethyl-phenylsulfaryl)-benzonitrile ([<sup>11</sup>C]DASB) is a positron emission tomography (PET) tracer that binds to the serotonin transporter (SERT) and can quantify regional serotonergic projection terminal density,<sup>12-14</sup> providing an opportunity to examine rostral serotonergic projection system terminal integrity in patients with MSA compared with PD.

## Methods

We conducted a single-center, observational, cross-sectional neuroimaging study to evaluate rostral brain [<sup>11</sup>C]DASB binding in MSA and compared these findings with existing DASB data available at the University of Michigan (UM) PET center from participants with PD. Patients were recruited from movement disorders clinics and through a web-based posting on a UM human subjects recruitment website (<https://umhealthresearch.org/>). All patients signed informed consent documents approved by the UM Medical Institutional Review Board.

Patients with MSA were aged 30 to 80 years with a diagnosis of possible or probable MSA-P or MSA-C according to the MSA Second Consensus Criteria<sup>15</sup> and had a Mini-Mental State Examination score of 24 or greater. Patients with PD were aged 45 years or older with modified Hoehn and Yahr stages 1 to 4 and met

the UK Brain Bank Clinical Diagnostic Criteria for PD.<sup>16</sup> PET data on the patients with PD in this cohort has been reported previously.<sup>17</sup> We excluded patients with contraindications to magnetic resonance imaging or PET imaging and those taking serotonergic or anticholinergic medications in the 2 months preceding enrollment. For comparison to both PD and MSA, we included [<sup>11</sup>C]DASB data obtained from our PET center on a group of healthy controls (HCs).

All patients underwent [<sup>11</sup>C]DASB PET imaging. Methods for our group's [<sup>11</sup>C]DASB approach are detailed elsewhere.<sup>17,18</sup> Briefly, we injected patients with an intravenous bolus followed by an 80-minute infusion of [<sup>11</sup>C]DASB. PET images were motion corrected and normalized into a common atlas space using NeuroStat software (<https://neurostat.neuro.utah.edu>). We defined volumes of interest (VOIs), including Brodmann areas and subcortical gray matter structures, on PET images using a Talairach brain atlas.<sup>19</sup> These brain regions were identified on normalized parametric K<sub>1</sub> PET images using a set of predefined Talairach atlas regions through the NeuroStat software package (additional details on this approach are described elsewhere<sup>20,21</sup>). We used equilibrium modeling to estimate the distribution volume in each voxel. Distribution volume ratios (DVRs) were calculated as a mean for each set of paired right and left hemisphere VOIs. We similarly calculated the mean of right and left brainstem VOIs including the medulla, raphe pontis, dorsal raphe, and substantia nigra. Given the potential for the confounding influence of partial volume effects in the cerebellum in an MSA cohort, a disorder characterized by regional cerebellar atrophy, we used superior supratentorial white matter as a normalization reference region for calculating individual patients' [<sup>11</sup>C]DASB DVR. We selected this region because it had a relatively lower level of [<sup>11</sup>C]DASB binding, not differing significantly between patients with PD and MSA. Another PET imaging group used a similar approach and reported low reference region SERT binding.<sup>22</sup>

We explored differences in intergroup DVRs in several different VOIs. The medulla, raphe pontis, dorsal raphe, substantia nigra, ventral striatum, ventral anterior cingulate cortex (Brodmann Area 24), and thalamus were defined on atlas images. Distinct from the ventral striatum, we defined the dorsal striatum VOI as the voxel-adjusted mean of the bilateral caudate nucleus and putamen. Limbic cortex was defined using the amygdala, hippocampus, and insula VOIs. The total cerebral cortex was defined using voxel-adjusted volumes specific to relevant Brodmann areas and limbic regions identified on the NeuroStat atlas, and the thalamic VOI was identified through the Talairach atlas. We used descriptive statistics to display the means and proportions between the MSA, PD and HC groups. We used two-sample *t* tests to compare patients with MSA

and PD in each of these VOIs. We conducted exploratory analyses within PD and MSA groups to evaluate for bivariate correlations (Pearson's *r*) between regional [<sup>11</sup>C]DASB DVR and clinical scales, including the Movement Disorders Society Revised Unified Parkinson's Disease Rating Scale (MDS-UPDRS) motor examination, the Montreal Cognitive Assessment (MoCA), the Geriatric Depression Scale (GDS), and the Epworth Sleepiness Scale (ESS).

## Results

A total of 59 patients consented to participate in the study, but we excluded two patients from analysis (one patient with MSA who could not complete the [<sup>11</sup>C]DASB scan and one patient with MSA who was taking a serotonergic medication), leaving a total cohort of 57 (23 patients with PD, 18 patients with MSA, and 16 HCs). In the MSA group, there were 10 patients with MSA-C and eight patients with MSA-P. We found no intergroup differences in any of the regions of interest (ROIs) on [<sup>11</sup>C]DASB PET imaging between the two MSA subtypes, so they were subsequently combined into one group for comparison with PD (Table 1).

Table 1 shows the differences between the groups in mean [<sup>11</sup>C]DASB DVRs in the selected ROIs. As expected, [<sup>11</sup>C]DASB binding in the cortical VOIs was higher in the HC group compared with patients with PD or MSA. Interestingly, the HCs showed a lower range of [<sup>11</sup>C]DASB binding in the striatum, ventral striatum, substantia nigra, dorsal raphe, and raphe pontis. There were no significant differences between patients with PD and MSA in total cortical, striatal, or substantia nigra [<sup>11</sup>C]DASB DVRs. Patients with MSA showed significantly lower [<sup>11</sup>C]DASB DVRs in the thalamus, limbic cortex, ventral striatum, raphe pontis, and medulla compared with patients with PD. Figure 1 depicts the [<sup>11</sup>C]DASB binding overlap between patients with MSA and PD in many supratentorial regions with qualitatively lower [<sup>11</sup>C]DASB binding in MSA in the limbic cortex and caudal brainstem. There were no sex differences seen in the PD group or in the MSA group in [<sup>11</sup>C]DASB DVR in any of the ROIs.

Patients with MSA and PD did not differ in MDS-UPDRS motor exam, MoCA, GDS, or ESS scores (Table 1). Correlations between these clinical variables and regional [<sup>11</sup>C]DASB DVRs are presented in Tables S1 and S2. Given the potential for inflated type 1 error due to multiple comparisons, these bivariate correlations are intended to be interpreted as hypothesis generating in nature. For the most part, the MoCA, GDS, and ESS scores did not show a consistent correlative pattern with [<sup>11</sup>C]DASB DVR in either patients with PD or MSA. Interestingly, patients with MSA showed an inverse correlation between elevated MDS-

**TABLE 1** Cohort characteristics and regional [<sup>11</sup>C]DASB DVRs

|                                     | PD, n = 23  | MSA, n = 18                   | Healthy controls, n = 16 comparing PD to MSA | $\chi^2/t$ test. <i>P</i> value |
|-------------------------------------|---|-------------------------------|--|---------------------------------|
| Age, years                          | 66.2 (6.7)  | 59.6 (7.6)                    | 66.0 (5.2)                                   | $t = 2.932, P = 0.006$          |
| Sex                                 | Female = 6, male = 17   | Female = 8, male = 9          | Female = 10, male = 6                        | $\chi^2 = 1.89, P = 0.17$       |
| Disease duration, years             | 4.9 (4.1) [range, 1–12 years]                                       | 2.9 (2.8) [range, 1–11 years] | –  | $t = 1.713, P = 0.095$          |
| Modified HY scale                   | HY1 (n = 2), HY1.5 (n = 4), HY2 (n = 9), HY2.5 (n = 6), HY3 (n = 2) | –                             | –  |                                 |
| MDS-UPDRS motor exam score          | 25.522 (9.050)  | 30.25 (19.033) [n = 14]       | –  | $t = 1.023, P = 0.314$          |
| Montreal Cognitive Assessment score | 25.565 (2.352)  | 24.333 (4.451) [n = 15]       | –  | $t = 1.115, P = 0.272$          |
| Geriatric Depression Scale score    | 7.217 (4.512)   | 8.857 (4.504) [n = 14]        | –  | $t = 1.073, P = 0.291$          |
| Epworth Sleepiness Scale score      | 6.826 (4.141)   | 6.571 (3.877) [n = 14]        | –  | $t = 0.186, P = 0.854$          |
| Region of interest                  |   |                               |  |                                 |
| Total cortex                        | 1.267 (0.130)   | 1.232 (0.093)                 | 1.792 (0.136)                                | $t = 0.964, P = 0.341$          |
| Caudate and putamen                 | 2.232 (0.182)   | 2.210 (0.192)                 | 2.007 (0.175)                                | $t = 0.379, P = 0.707$          |
| Thalamus                            | 2.381 (0.209)   | 2.187 (0.164)                 | 2.103 (0.236)                                | $t = 3.243, P = 0.002$          |
| Limbic cortex                       | 1.553 (0.130)   | 1.454 (0.138)                 | 1.799 (0.144)                                | $t = 2.365, P = 0.023$          |
| Ventral striatum                    | 2.388 (0.194)   | 2.205 (0.241)                 | 1.959 (0.178)                                | $t = 2.702, P = 0.010$          |
| Ventral anterior cingulate          | 1.384 (0.115)   | 1.360 (0.117)                 | 1.650 (0.137)                                | $t = 0.656, P = 0.516$          |
| Substantia nigra                    | 2.416 (0.360)   | 2.401 (0.346)                 | 1.614 (0.173)                                | $t = 0.138, P = 0.891$          |
| Dorsal raphe                        | 2.970 (0.342)   | 2.912 (0.390)                 | 1.700 (0.139)                                | $t = 0.509, P = 0.614$          |
| Raphe pontis                        | 2.566 (0.297)   | 2.241 (0.300)                 | 1.556 (0.253)                                | $t = 3.464, P = 0.001$          |
| Medulla                             | 1.571 (0.168)   | 1.364 (0.210)                 | 1.464 (0.189)                                | $t = 3.501, P = 0.001$          |

Values are expressed as mean (standard deviation); absolute values of  $t$  test/ $\chi^2$  are presented.

Abbreviations: [<sup>11</sup>C]DASB, [<sup>11</sup>C]3-amino-4-(2-dimethylaminomethyl-phenylsulfanyl)-benzonitrile; DVR, distribution volume ratio; PD, Parkinson's disease; MSA, multiple system atrophy; HY, Hoehn and Yahr; MDS-UPDRS, Movement Disorders Society Revised Unified Parkinson's Disease Rating Scale.

UPDRS scores and lower [<sup>11</sup>C]DASB DVRs seen in multiple different brain regions (Fig. S1). Outside of the striatum, these associations were not seen in patients with PD. Clinical data were available for only four of the eight total patients with MSA-P, limiting our ability to conduct MSA subtype-specific analyses. Even so, among the 10 patients with MSA-C with available clinical data, similar patterns of inverse correlations were seen between MDS-UPDRS motor score and [<sup>11</sup>C]DASB DVR, including in the total cortex ( $r = -0.7140, P = 0.0204$ ), striatum ( $r = -0.7054, P = 0.0227$ ), ventral striatum ( $r = -0.7457, P = 0.0133$ ), and ventral anterior cingulate

( $r = -0.7930, P = 0.0062$ ), but not in any of the other ROIs.

## Discussion

Relative to the participants with PD, the participants with MSA showed comparable levels of [<sup>11</sup>C]DASB binding in neocortical and dorsal striatal ROIs but lower [<sup>11</sup>C]DASB DVRs in key subcortical regions, including the thalamus, ventral striatum, and limbic cortex as well as greater reductions in caudal brainstem [<sup>11</sup>C]DASB binding in the raphe pontis and medulla.

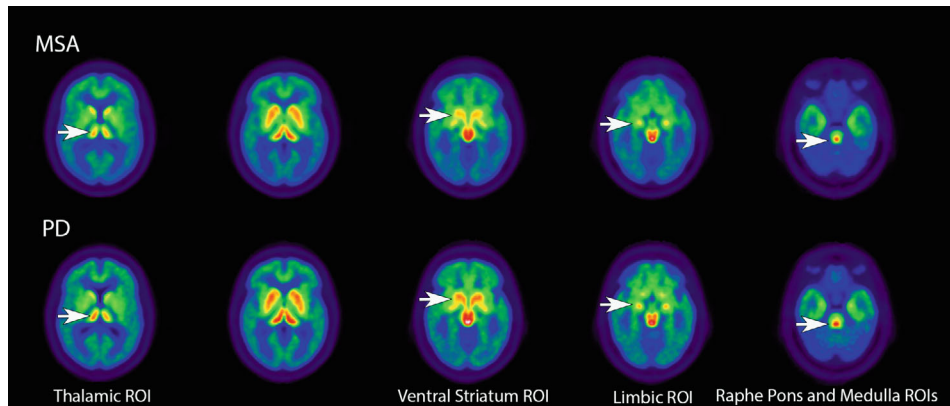


**FIG. 1.** Axial images presenting group averages for [<sup>11</sup>C]3-amino-4-(2-dimethylaminomethyl-phenylsulfuryl)-benzonitrile (DASB) positron emission tomography in patients with MSA and PD. White arrows in the top rows show reduced [<sup>11</sup>C]DASB binding in MSA compared with PD in several ROIs. MSA, multiple system atrophy; PD, Parkinson's disease; ROI, region of interest.

Patients with MSA and PD showed lower cortical [<sup>11</sup>C]DASB binding compared with the HCs but higher striatal, midbrain, and pontine [<sup>11</sup>C]DASB binding. These MSA/PD region-specific findings may reflect the presence of compensatory physiology in subcortical serotonergic systems. Lower [<sup>11</sup>C]DASB binding in patients with MSA in various brain regions correlated with greater motor impairment on the MDS-UPDRS motor exam. Our findings are from a relatively small cohort and may very well be impacted by multiple comparisons. For this important reason, they require replication in independent data sets. Nevertheless, these data comprise the first [<sup>11</sup>C]DASB study in MSA. Our findings confirm the presence of lower brainstem serotonergic pathology in MSA and raise the possibility of relatively selective rostral serotonergic network abnormalities as a distinctive pathological feature of MSA.

The rostral serotonergic raphe complex, located in the midbrain/rostral pons, gives rise to two distinct groups of ascending fibers—the dorsal and ventral/median raphe pathways. The dorsal raphe projects to the striatum and globus pallidus, whereas the ventral/median raphe sends projections to other forebrain regions, including the thalamus, hypothalamus, and limbic structures. Previous neuropathological studies demonstrated advanced serotonergic neurodegeneration in the medullary raphe complex of patients with MSA,<sup>6,7,23</sup> a result consistent with our [<sup>11</sup>C]DASB PET findings. In contrast to the marked caudal brainstem serotonergic neuron loss, a separate postmortem study showed only mild degeneration of the midbrain dorsal and median raphe complex in MSA, comprising an intermediate stage between HCs and more severe findings found in patients with Lewy body dementia.<sup>24</sup> In this latter postmortem study, the patients with MSA had a mean disease duration of 7 years. Our study expands on these findings by

characterizing serotonergic system changes in participants with MSA with an average disease duration of only 3 years. The *in vivo* SERT density measurements of the cortex and dorsal striatum in our patients with MSA was similar to PD and consistent with prior post-mortem findings. Our finding of comparable *in vivo* serotonin transporter density in the cortex and dorsal striatum in patients with MSA and PD could support the conclusion that abnormalities of some key serotonergic projections are similar in PD and MSA. We found significant differences in some regions, suggesting differential loss of serotonergic terminals and perikarya. Alternatively, SERT expression might be differentially regulated in PD and MSA, possibly reflecting differential compensatory capacity of serotonergic systems in these two disorders. Longitudinal studies using multiple serotonergic tracers are needed to clarify what PET findings reflect degenerative terminal loss versus endogenous compensatory responses.

Interestingly, patients with MSA and PD showed lower cortical but higher basal ganglia, midbrain, and pontine [<sup>11</sup>C]DASB DVRs compared with controls. There are several possible explanations for these intergroup findings, including the possibility that the serotonergic system may show unique compensatory features in synucleinopathies. Prange and colleagues recently reported increased [<sup>11</sup>C]DASB binding in the ventral striatum and anterior cingulate cortex of patients with PD with apathy, suggesting that regional [<sup>11</sup>C]DASB elevations may occur in the setting of local neurodegeneration.<sup>25</sup> Another possibility is that rising SERT density is not simply a synaptic phenomenon but might also carry an autoregulatory role in the proximal cell bodies of serotonergic projection neurons. An electrophysiologic study has shown that local application of selective serotonin reuptake inhibitors to the dorsal raphe nucleus of mice leads to local SERT inhibition at the level of the cell bodies and subsequent

enhancement of synaptic serotonin release.<sup>26</sup> A third possibility is that our use of the superior supratentorial white matter as a reference region may have affected intergroup comparisons. This approach has not been reported or studied previously for [<sup>11</sup>C]DASB. We chose this region rather than the cerebellar [<sup>11</sup>C]DASB reference region given the potential for cerebellar pathology in MSA to bias intergroup comparisons. It is worth noting, however, that supratentorial white matter pathology has been described in MSA compared with controls.<sup>27</sup> As such, this region may not be free of bias. Prospective validation of this approach against a model dependent on arterial sampling will be needed moving forward.

These results showing elevated regional [<sup>11</sup>C]DASB binding in PD compared with controls in the rostral brainstem and basal ganglia contrast with those reported in other cohorts.<sup>8,28</sup> At least one PD study suggests that certain subcortical regions may show declines in [<sup>11</sup>C]DASB binding with advancing disease duration.<sup>29</sup> Nevertheless, the story of how regional [<sup>11</sup>C]DASB binding changes in PD is more nuanced and does not fit a monotonic, unidirectional pattern. Paradoxical elevations in [<sup>11</sup>C]DASB binding in the hypothalamus and hippocampus compared with controls have been reported in PD,<sup>30</sup> as have paradoxical [<sup>11</sup>C]DASB upregulations in patients with PD and depression in the amygdala, hypothalamus, caudal raphe nuclei, and posterior cingulate cortex.<sup>31</sup> Differences in published [<sup>11</sup>C]DASB PD findings most likely reflect the complicated influence of baseline differences in serotonergic integrity and genetic risk factors, variability across cohorts in disease duration, previous use of drugs relevant to the serotonergic nervous system, and heterogeneity of clinical features known to correlate with serotonergic pathology. A multicenter, PD observational study involving multiple serotonergic tracers would be the optimal next step to better understanding the natural history of [<sup>11</sup>C]DASB bindings in synucleinopathies.

Our exploratory clinical correlative analyses showed an MSA-specific inverse correlation between the severity of motor impairment and serotonergic integrity in several different cortical, basal ganglia, and brainstem ROIs. This is a novel finding and suggests that serotonergic degeneration may be a possible therapeutic target for motor progression in MSA. Our findings are potentially confounded by the possibility of type 1 error and should be interpreted cautiously.

In addition to its cross-sectional design, another relevant limitation of our study is its lack of a uniform clinical assessment battery; the patients with MSA and PD were recruited and imaged through different clinical research protocols. MSA and PD are known to have overlapping clinical features but distinctive disease-specific clinical factors possibly related to the

serotonergic system dysfunctions. We were also missing clinical data in four patients with MSA-P. Patients with PD were on average 6.6 years older than patients with MSA and had a mean disease duration that was 2 years longer. These findings may very well have impacted the results of our study. For example, it is possible that the clinical correlations seen between MDS-UPDRS scores and [<sup>11</sup>C]DASB DVRs in patients with MSA only reflect dynamic changes seen in early disease that reach a ceiling effect as disease duration advances. The higher overall MDS-UPDRS scores seen in patients with MSA in our cohort though would argue slightly against the possibility that patients with MSA may have less advanced parkinsonism compared with patients with PD.

The potential of the ascending serotonergic projection system as a biomarker or therapeutic target in MSA is yet to be determined. Nevertheless, given the paucity of current MSA treatments and the clinical availability of serotonergic drugs targeting different 5HT receptor classes, understanding serotonergic system alterations in MSA and other synucleinopathies may have diagnostic and therapeutic relevance. The present study is a step toward elucidating serotonergic network dysfunction in this rare and complex disease. ■

### Data Availability Statement

The data that support the findings of this study are available from the corresponding author upon reasonable request.

### References

1. Braak H, Del Tredici K, Rub U, de Vos RA, Jansen Steur EN, Braak E. Staging of brain pathology related to sporadic Parkinson's disease. *Neurobiol Aging* 2003;24(2):197–211.
2. Giguere N, Burke Nanni S, Trudeau LE. On cell loss and selective vulnerability of neuronal populations in Parkinson's disease. *Front Neurol* 2018;9:455.
3. Miguez C, Morera-Herreras T, Torrecilla M, Ruiz-Ortega JA, Ugedo L. Interaction between the 5-HT system and the basal ganglia: functional implication and therapeutic perspective in Parkinson's disease. *Front Neural Circuits* 2014;8:21.
4. Valdinocci D, Radford RAW, Goulding M, Hayashi J, Chung RS, Pountney DL. Extracellular interactions of alpha-synuclein in multiple system atrophy. *Int J Mol Sci* 2018;19(12):4129.
5. Papp MI, Kahn JE, Lantos PL. Glial cytoplasmic inclusions in the CNS of patients with multiple system atrophy (striatonigral degeneration, olivopontocerebellar atrophy and shy-Drager syndrome). *J Neurol Sci* 1989;94(1–3):79–100.
6. Benarroch EE, Schmeichel AM, Low PA, Parisi JE. Involvement of medullary serotonergic groups in multiple system atrophy. *Ann Neurol* 2004;55(3):418–422.
7. Benarroch EE, Schmeichel AM, Low PA, Parisi JE. Depletion of putative chemosensitive respiratory neurons in the ventral medullary surface in multiple system atrophy. *Brain* 2007;130:469–475.
8. Wilson H, Giordano B, Turkheimer FE, Chaudhuri KR, Politis M. Serotonergic dysregulation is linked to sleep problems in Parkinson's disease. *Neuroimage Clin* 2018;18:630–637.

9. Maillet A, Krack P, Lhommée E, et al. The prominent role of serotonergic degeneration in apathy, anxiety and depression in de novo Parkinson's disease. *Brain* 2016;139(Pt 9):2486–2502.
10. Politis M, Loane C, Wu K, Brooks DJ, Piccini P. Serotonergic mediated body mass index changes in Parkinson's disease. *Neurobiol Dis* 2011;43(3):609–615.
11. Perez-Soriano A, Giraldo DM, Rios J, et al. Progression of motor and non-motor symptoms in multiple system atrophy: a prospective study from the Catalan-MSA registry. *J Parkinsons Dis* 2021;11(2): 685–694.
12. Houle S, Ginovart N, Hussey D, Meyer JH, Wilson AA. Imaging the serotonin transporter with positron emission tomography: initial human studies with [<sup>11</sup>C]DAPP and [<sup>11</sup>C]DASB. *Eur J Nucl Med* 2000;27(11):1719–1722.
13. Hummerich R, Reischl G, Ehrlichmann W, Machulla HJ, Heinz A, Schloss P. DASB -in vitro binding characteristics on human recombinant monoamine transporters with regard to its potential as positron emission tomography (PET) tracer. *J Neurochem* 2004;90(5):1218–1226.
14. Parsey RV, Kent JM, Oquendo MA, et al. Acute occupancy of brain serotonin transporter by sertraline as measured by [<sup>11</sup>C]DASB and positron emission tomography. *Biol Psychiatry* 2006;59(9):821–828.
15. Gilman S, Wenning GK, Low PA, et al. Second consensus statement on the diagnosis of multiple system atrophy. *Neurology* 2008;71(9): 670–676.
16. Hughes AJ, Daniel SE, Kilford L, Lees AJ. Accuracy of clinical diagnosis of idiopathic Parkinson's disease: a clinico-pathological study of 100 cases. *J Neurol Neurosurg Psychiatry* 1992;55(3):181–184.
17. Kotagal V, Spino C, Bohnen NI, Koeppe R, Albin RL. Serotonin, beta-amyloid, and cognition in Parkinson disease. *Ann Neurol* 2018;83(5):994–1002.
18. Kotagal V, Albin RL, Muller ML, et al. Symptoms of rapid eye movement sleep behavior disorder are associated with cholinergic denervation in Parkinson disease. *Ann Neurol* 2012;71(4):560–568.
19. Bohnen NI, Albin RL, Koeppe RA, et al. Positron emission tomography of monoaminergic vesicular binding in aging and Parkinson disease. *J Cereb Blood Flow Metab* 2006;26(9):1198–1212.
20. Minoshima S, Koeppe RA, Frey KA, Kuhl DE. Anatomic standardization: linear scaling and nonlinear warping of functional brain images. *J Nucl Med* 1994;35(9):1528–1537.
21. Frey KA, Minoshima S, Koeppe RA, Kilbourn MR, Berger KL, Kuhl DE. Stereotaxic summation analysis of human cerebral benzodiazepine binding maps. *J Cereb Blood Flow Metab* 1996;16(3): 409–417.
22. Buck A, Gucker PM, Schonbachler RD, et al. Evaluation of serotonergic transporters using PET and [<sup>11</sup>C](+)-McN-5652: assessment of methods. *J Cereb Blood Flow Metab* 2000;20(2):253–262.
23. Tada M, Kakita A, Toyoshima Y, et al. Depletion of medullary serotonergic neurons in patients with multiple system atrophy who succumbed to sudden death. *Brain* 2009;132:1810–1819.
24. Benarroch EE, Schmeichel AM, Sandroni P, Parisi JE, Low PA. Rostral raphe involvement in Lewy body dementia and multiple system atrophy. *Acta Neuropathol* 2007;114(3):213–220.
25. Prange S, Metereau E, Maillet A, et al. Limbic serotonergic plasticity contributes to the compensation of apathy in early Parkinson's disease. *Mov Disord* 2022;37(6):1211–1221.
26. Dankoski EC, Carroll S, Wightman RM. Acute selective serotonin reuptake inhibitors regulate the dorsal raphe nucleus causing amplification of terminal serotonin release. *J Neurochem* 2016;136(6): 1131–1141.
27. Wang PS, Yeh CL, Lu CF, Wu HM, Soong BW, Wu YT. The involvement of supratentorial white matter in multiple system atrophy: a diffusion tensor imaging tractography study. *Acta Neurol Belg* 2017;117(1):213–220.
28. Politis M, Wu K, Loane C, et al. Staging of serotonergic dysfunction in Parkinson's disease: an in vivo <sup>11</sup>C-DASB PET study. *Neurobiol Dis* 2010;40(1):216–221.
29. Maillet A, Météreau E, Tremblay L, et al. Serotonergic and dopaminergic lesions underlying parkinsonian neuropsychiatric signs. *Mov Disord* 2021;36(12):2888–2900.
30. Fu JF, Klyuzhin I, Liu S, et al. Investigation of serotonergic Parkinson's disease-related covariance pattern using [(11)C]-DASB/PET. *Neuroimage Clin* 2018;19:652–660.
31. Politis M, Loane C. Serotonergic dysfunction in Parkinson's disease and its relevance to disability. *Sci World J* 2011;11:1726–1734.

## Supporting Data

Additional Supporting Information may be found in the online version of this article at the publisher's web-site.